Modification of Source Strength in Low-Dose-Rate Lung Brachytherapy with ^{125}I and ^{103}Pd Seeds

Rezaei H.[1], Mostaghimi H.[2,3]*, Mehdizadeh A. R.[2,3]

[1]Department of Radiology, School of Paramedical Sciences, Shiraz University of Medical Sciences, Shiraz, Iran
[2]Department of Biomedical Physics and Engineering, School of Medicine, Shiraz University of Medical Sciences, Shiraz, Iran
[3]Advanced Health Technologies Research Center, Shiraz University of Medical Sciences, Shiraz, Iran

ABSTRACT

Background: A new treatment approach for most patients who have undergone early stage non-small-cell lung carcinoma (NSCLC) is wedge resection plus permanent implant brachytherapy. However, the specification of dose to medium at low energies especially in heterogeneous lung is unclear yet.

Objective: The present study aims to modify source strength for different configurations of ^{125}I and ^{103}Pd seeds used in lung permanent implant brachytherapy.

Methods: Different arrays of ^{125}I and ^{103}Pd seeds were simulated by MCNPX code in protocol-based water vs. actual 3D lung environments. Absorbed dose was, then, scored in both mediums. Dose differences between both environments were calculated and source strength was modified for the prescription point. In addition, lung-to-water absorbed dose ratio was obtained and presented by precise equations.

Results: Due to significant differences in prescription dose, source strength was modified 16%-19% and 37%-43% for different configurations of ^{125}I and ^{103}Pd seeds, respectively. In addition, depth-dependent dose differences were observed between the actual lung and protocol-based water mediums (dose difference as a function of depth).

Conclusion: Modification of source strength is essential for different arrangements of ^{125}I and ^{103}Pd seeds in lung implantation. Modified source strength and presented equations are recommended to be considered in future studies based on lung brachytherapy.

Keywords

^{125}I seed, ^{103}Pd Seed, Lung Permanent Implant Brachytherapy, Monte Carlo Method

Introduction

Lung cancer has the highest rate of mortality among all cancers with more than 80% diagnosis of non-small-cell lung carcinoma (NSCLC) [1, 2]. A new treatment approach for a wide range of high-risk patients with early-stage NSCLC who do not have proper respiratory conditions for lobectomy or pneumonectomy is wedge resection plus low-dose-rate (LDR) permanent implant brachytherapy [3, 4, 5]. In this technique, a wedge-shaped piece of lung is removed by segmentectomy, and an implant is created by weaving strands of LDR seeds (e.g. ^{125}I or ^{103}Pd) into a vicryl mesh which is then sutured over the resection staple line with the goal of delivering 100 to 120 Gy to the prescription point, 5 mm above the seeds plane [6, 7]. The implants are

*Corresponding author:
H. Mostaghimi
Department of Biomedical Physics and Engineering, School of Medicine, Shiraz University of Medical Sciences, Shiraz, Iran; Advanced Health Technologies Research Center, Shiraz University of Medical Sciences, Shiraz, Iran
E-mail: mostaghimi@sums.ac.ir

Received: 10 May 2017
Accepted: 27 June 2017

prepared specifically for each patient under the supervision of treatment planning team in different configurations [8, 9]. This technique was first used at the end of the 1990s and initially described by Chen et al. [9, 10]. Chen et al. applied different configurations of ^{125}I seeds (mostly 40, 50 and 60 seeds) for the mean target area of 48 cm^2 with the mean total activity of 22 mCi and have reported this technique potentially effective and well tolerated with no increase in postoperative complications. Other researchers have also reported similar results and excellent local control rate; with seeds array as large as 50 cm^2 [4, 11]. Johnson et al. [8] have reported a monogram for different configurations of seeds with proper arrays. American Association of Physicists in Medicine Task Group number 43 (AAPM TG-43U1 protocol) recommends initial source strength (initial air-kerma strength) based on water-equivalent homogenous tissue [12, 13] while lung heterogeneity and difference of lung-water electron densities (1:4) can cause significant dose change especially in case of multiple seeds [13]. Although, according to the recent multi-societal TG-186 report, assuming the patient as water being dosimetrically incorrect, AAPM TG-43 is still a commonly recommended protocol. Based on ICRU recommendation, the uncertainty of dose determination should not exceed 5% which only 2% can be due to calculations error [14]; and a study conducted by Van Dyk has reported 22% increase in the occurrence of radiation pneumonitis due to 5% increase in lung absorbed dose [15]. Sutherland [16] has studied breast and lung permanent brachytherapy using the BrachyDose algorithm and reported about 20% dose difference at the prescription point for different configurations of ^{125}I seeds. Since the dosimetry in the actual lung is impractical, and accurate dose distribution is crucial for optimized treatment, in this study we intend to simulate water-equivalent and 3D lung environments and four configurations of ^{125}I and ^{103}Pd seeds in order to calculate the absorbed dose and dose difference caused by differences between protocol presumption and actual lung. Mentioned configurations were chosen based on previous studies conducted by Chen [8], Johnson [9] and Sutherland [16]. In the end, we present modified source strength (initial air-kerma strength) and precise equations in order to be considered in future studies based on lung permanent implant brachytherapy.

Material and Methods

Radiation Transport

In this study, a Monte Carlo N- Particle transport code (MCNPX, version 2.6.0) was used to simulate thorax phantom and four configurations of ^{125}I and ^{103}Pd seeds in order to calculate the lung absorbed dose and to modify seeds initial strength calculated by considering AAPM TG-43 U1 recommendations. With regard to the energy range of ^{125}I and ^{103}Pd sources and the voxels size (1 mm^3 cubic voxel), electron equilibrium exists and collision kerma is a good estimation of absorbed dose. F6 track-length estimator was used to obtain dose per history and converted to total absorbed dose rate (for 40, 50 and 60 seeds) by equation 1 [16]. For permanent implant brachytherapy, the total absorbed dose at each voxel can be obtained by multiplying the total absorbed dose rate by mean lifetime (τ =

$$\text{Total Absorbed Dose Rate (cGy/h)} = \text{MC output (MeV/gr per photon)} \times \frac{1}{S_k}[\,(\text{cm}^2.\text{MeV/gr per photon})^{-1} \times S_k\,(\text{U/seed}) \times N_s \qquad (1)$$

1.443 $T_{1/2}$) of brachytherapy source.

where MC output is the F6 tally output (dose per history), s_k is air-kerma strength per history obtained from Monte Carlo calculations, S_k is the initial air-kerma strength of each source in the treatment [17] and N_s is the total number of seeds in each particular configuration. The calculation of air kerma strength per history (s_k) for a particular seed is thoroughly described by Taylor et al. [18]. The photon and electron cut-off energies were set to 5 and 10 keV, respectively. In order to reach maximum accuracy (max error 1%), 1.5×10^9 photon histories were considered.

Simulated Thorax Phantom

Using quadric equations, anthropomorphic QRM thorax phantom including lung, heart and vertebral column was simulated by MCNPX 2.6.0 considering their constituent compositions and densities. These phantoms are generally made in the form of elliptical cylinders as thorax with a cross-section of 20×30 cm^2 including two symmetric elliptical cylinders as lungs with a cross-section of 12×16 cm^2. Heart and vertebral column were simulated as circular cylinders with proper constituent compositions. A part of the right lung with 50 cm^2 cross-section was removed as the resected volume, and the seeds' plane was simulated on it. The composition and densities of thorax organs are mentioned in Table 1 [19, 20]. Figure 1 illustrates the cross-section of simulated anthropomorphic QRM thorax phantom.

^{125}I Seed (Amersham, model 6711)

In this study, ^{125}I source (model 6711) was used. This source was benchmarked by Monte Carlo simulation in our previous study and was simulated thoroughly based on 3D actual source [21]. In designing the source, one silver cylindrical marker was used by 10.5 g/cm^3 density, 2.8 mm length and 0.254 mm radius covered with Br_5I_2 compound with 2 µm thickness and 6.245 g/cm^3 density. Source effective length was 2.8 mm and the end of the source was curved by 0.045 mm under 45-degree angles. This composition was located at one titanium capsule with 4.54 g/cm^3 density filled by Argon gas with 1.784 g/cm^3 density. The average energy, half-life and mean life-time of ^{125}I source are 28.37 keV, 59.4 and 85.7 days, respectively [22, 23].

^{103}Pd Seed (Theragenics, model 200)

^{103}Pd seed (Theragenics, model 200) includes two cylindrical graphite rods with 2.22 g/cm^3 density, 0.56 mm diameter and 0.890 mm length. These rods are coated with a thin layer of radioactive palladium with 12.03 g/cm^3 density and 2.2 µm thickness. The graphite cylinders are separated by a lead marker with 11.4 g/cm^3 density, 0.5 mm diameter and 1.09 mm length. Mentioned components are capsulated inside a cylindrical titanium capsule with 4.51 g/cm^3 density, 0.826 mm

Table 1: Mass densities and elemental compositions of thorax tissues used in our simulations [19, 20]

Material	Composition (mass %)					ρ
	H	C	N	O	Elements with Z > 8	(g/cm³)
Lung	10.3	10.5	3.1	74.9	Na(0.2), P(0.2), S(0.3), Cl(0.3), K(0.2)	0.26
Heart	10.3	12.1	3.2	73.4	Na(0.1), P(0.1), S(0.2), Cl(0.3), K(0.2), Fe(0.1)	1.06
Vertebrae	3.4	15.5	4.2	43.5	Na(0.1), Mg(0.2), P(10.3), S(0.3), Ca(22.5)	1.92
Soft Tissue	10.2	11.2	3.0	74.5	Na(0.1), P(0.2), S(0.3), Cl(0.1), K(0.4)	1.05
Water	11.22	0.0	0.0	88.78	_	0.998
Air(TG-43)	0.07	0.01	75.03	23.61	Ar(1.27)	0.0012

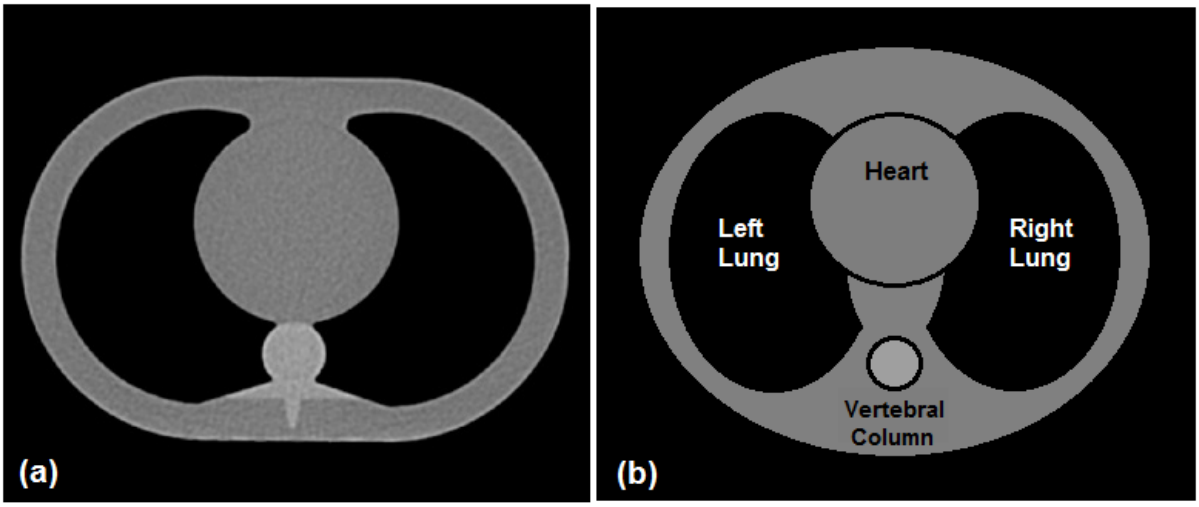

Figure 1: a. Cross section of anthropomorphic QRM thorax phantom. b. Thorax Phantom Simulated in this study by MCNPX code.

external diameter and 0.056 mm thickness. Both ends of the capsules are closed with cylindrical titanium cups as shields. These cups have 0.306 mm internal diameter and 0.04 mm thickness. The total length of this source is 4.5 mm with 4.23 mm effective length. The average energy, half-life and mean life-time of the ^{103}Pd source are 20.74 keV, 16.99 and 24.5 days, respectively. ^{103}Pd seed (Theragenics, model 200) was benchmarked and its dosimetric parameters have been reported by the present authors previously [24].

Mesh Including 40, 50 and 60 Seeds

Lung mesh seed implants can be used to cover a target area of about 50 cm^2 [4, 9, 11]. Four configurations of ^{125}I and ^{103}Pd seeds considered in this study are mentioned in Table

Table 2: Initial air-kerma strength per seed (U/seed) per prescription dose (100 Gy) for different configurations of ^{125}I and ^{103}Pd seeds. $(TG\text{-}43)_{sim}$ is calculated source strength based on AAPM TG-43 U1 protocol (in water environment) versus source strength modified by authors based on actual 3D lung environment.

Configuration		Row Spacing (cm)	Initial source strength (U/prescription dose)					
			^{103}Pd (200)			^{125}I (6711)		
			$(TG\text{-}43)_{Sim}$	Modified by Authors	%Diff (Rounded)	$(TG\text{-}43)_{Sim}$	Modified by Authors	%Diff (Rounded)
I	(4 × 10)	1.5	5.04	2.88	-42 %	0.75	0.61	-18 %
II	(4 × 10)	1.3	4.24	2.53	-40 %	0.67	0.56	-16 %
III	(5 × 10)	1.0	3.03	1.90	-37 %	0.48	0.41	-15 %
IV	(6 × 10)	0.8	2.50	1.58	-36 %	0.39	0.33	-16 %

2. These configurations were chosen based on previous studies done by Chen et al. [8], Johnson et al. [9] and Sutherland et al. [16]. Ten seeds were put in each row with 1 cm center-to-center distance but with various row spacing (RS) due to row numbers. Row spacing was 0.8, 1, 1.3 and 1.5 cm for 60, 50, 40(I) and 40(II) seeds configurations, respectively. Figure 2 shows configurations II and IV with 40 and 60 seeds, both on a 5×10 cm^2 plane but with different row spacing. Using equation 1, initial source strength was calculated in the water-equivalent environment (based on AAPM TG-43U1 protocol) to deliver 100 Gy to the prescription point. In this study, the plane with 5×10 cm^2 cross-section was considered as the resected volume of the lung.

Absorbed Dose & Dose Difference

The purpose of putting mesh including LDR seeds is to deliver 100 to 120 Gy dose to the prescription point 5 mm above center, perpendicular to the plane. This point is illustrated in Figure 3. Since the treatment time in permanent implant brachytherapy is the same for different cases (source mean lifetime) the comparison of absorbed dose rate and absorbed dose is equivalent. To obtain depth dose with high resolution, 50 cubic voxels with 1 mm^3 volume were considered on the central axis in a 5 cm depth. Using equation 1 and F6 tally outputs in a water environment initial strength per seed was calculated for each configuration in order to deliver 100 Gy to the prescription point. Mentioned source strength was used to calculate prescription dose in lung environment (using MC output in lung environment). Due to significant differences, source initial strength was modified by authors so that prescription dose difference between water and lung environments became almost zero (<0.5%). $D_{W(TG-43)}$ and $D_{L(TG-43)}$ are absorbed dose rates in water-equivalent and actual lung tissues by application of seed strength based on TG-43U1 protocol, respectively. $D_{L(Mod)}$ is lung absorbed dose rate considering modified source strength presented in this study. The maximum error in dose calculation was below 0.5% at the first 2 cm and below 1% between 2 to 5 cm. The percentage dose differences between two cases were calculated as below:

$$\%Diff = [(D_L - D_W) / D_W] \times 100 = [(D_L / D_W) - 1] \times 100 \qquad (2)$$

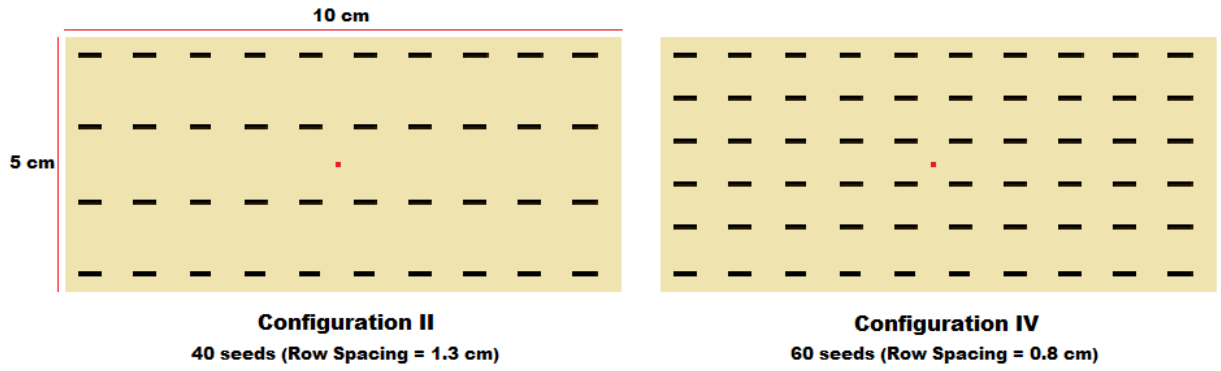

Figure 2: Configuration II (40 seeds) versus configuration IV (60 seeds). All configurations are simulated on a 5×10 cm^2 plane; ten seeds in each row with 1 cm center-to-center distance but with various row spacing.

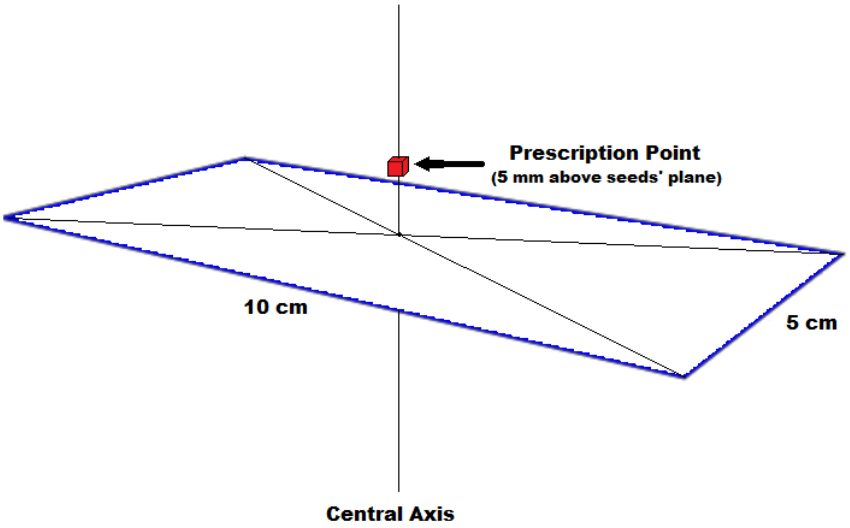

Figure 3: Prescription point at the center of red cube (voxel) at 0.5 cm along central axis of seeds' plane. The voxel dimension is 1×1×1 mm^3.

where D_L and D_W are the absorbed dose rates of a particular voxel in lung and water-equivalent tissues, respectively. The percentage dose difference in lung between two situations (water-based vs. modified source strength) is calculated with a similar equation.

Results and Discussion

Multiple MCNP programs were programmed and implemented for different cases mentioned in the article. Different configurations of ^{125}I and ^{103}Pd seeds were simulated in protocol-based water-equivalent vs. actual lung environments and F6 tally outputs were obtained from 50 cubic voxels along central axis up to 5 cm depth. Using equation 1 and specific treatment time, the prescription dose was considered as 100 Gy in water environment (based on protocol) and source initial strength was obtained for 40, 50 and 60 seeds configurations. Protocol-based source strength is shown in Table 2 (labeled as AAPM TG-43) for various configurations of ^{125}I and ^{103}Pd seeds.

By using mentioned source strength, the total absorbed dose rate of each voxel (depth) was calculated by equation 1 in water ($D_{W(TG-43)}$) and lung ($D_{L(TG-43)}$) up to 5 cm depth. Significant differences in prescription dose were observed for different cases so that lung prescription dose ($D_{L(TG-43)}$ at d = 0.5 cm) was 23.2%, 20.8%, 18.2% and 18.6% higher than protocol recommendation ($D_{W(TG-43)}$ at d = 0.5 cm) for configurations I, II, III and IV of ^{125}I seeds , respectively. Mentioned differences were 75.7%, 67.4%, 58.2% and 58.6% for configurations I, II, III and IV of ^{103}Pd seeds, respectively. Therefore, protocol-based initial strength was modified by the present authors to new figures (Table 2) so that prescription dose differences between water and lung environments reached almost zero (< 0.5%) in all cases. Lung absorbed dose rate was also calculated with modified source strength,

Table 3: Total absorbed dose rate (cGy.h^{-1}) as function of distance for different configurations of ^{125}I seeds in water and lung environments calculated by equation 1.

Depth (cm)	Total Absorbed Dose Rate (cGy/h)											
	$D_{W(TG-43)}$				$D_{L(TG-43)}$				$D_{L(Mod)}$			
	I	II	III	IV	I	II	III	IV	I	II	III	IV
0.1	5.74	5.93	5.01	6.12	7.07	7.14	5.64	7.06	5.75	5.93	4.75	5.92
0.2	5.63	5.77	5.70	5.99	6.81	6.85	6.43	6.87	5.54	5.69	5.41	5.76
0.3	5.38	5.54	5.66	5.64	6.49	6.56	6.47	6.55	5.28	5.45	5.45	5.49
0.4	5.12	5.20	5.35	5.26	6.27	6.22	6.20	6.14	5.10	5.16	5.22	5.15
0.5	**4.82**	**4.89**	**4.90**	**4.84**	**5.94**	**5.91**	**5.79**	**5.74**	**4.83**	**4.90**	**4.88**	**4.82**
0.6	4.53	4.54	4.48	4.43	5.65	5.57	5.40	5.33	4.59	4.63	4.54	4.47
0.7	4.23	4.21	4.07	4.07	5.34	5.25	5.00	4.97	4.35	4.36	4.21	4.17
0.8	3.93	3.90	3.70	3.70	5.02	4.92	4.64	4.65	4.08	4.09	3.91	3.90
0.9	3.62	3.58	3.39	3.39	4.74	4.62	4.34	4.29	3.86	3.84	3.65	3.60
1.0	3.39	3.31	3.10	3.15	4.48	4.33	4.03	4.03	3.64	3.59	3.39	3.38
1.1	3.14	3.07	2.86	2.87	4.23	4.08	3.80	3.80	3.44	3.38	3.20	3.19
1.2	2.91	2.83	2.63	2.64	3.99	3.84	3.56	3.57	3.25	3.19	3.00	2.99
1.3	2.71	2.60	2.43	2.44	3.78	3.59	3.36	3.35	3.08	2.98	2.83	2.81
1.4	2.51	2.44	2.25	2.26	3.58	3.42	3.14	3.17	2.91	2.84	2.64	2.66
1.5	2.33	2.24	2.08	2.06	3.41	3.22	2.97	2.95	2.78	2.67	2.50	2.48
1.6	2.15	2.09	1.93	1.91	3.25	3.07	2.82	2.78	2.64	2.55	2.37	2.34
1.7	2.00	1.95	1.79	1.78	3.06	2.89	2.67	2.63	2.49	2.40	2.25	2.21
1.8	1.89	1.82	1.67	1.66	2.93	2.74	2.53	2.49	2.38	2.28	2.13	2.09
1.9	1.77	1.70	1.54	1.55	2.77	2.61	2.40	2.35	2.25	2.17	2.02	1.97
2.0	1.65	1.58	1.45	1.43	2.65	2.46	2.28	2.23	2.15	2.05	1.92	1.87
2.1	1.53	1.47	1.34	1.33	2.50	2.35	2.14	2.13	2.03	1.95	1.80	1.79
2.2	1.44	1.36	1.24	1.25	2.38	2.24	2.04	2.04	1.94	1.86	1.72	1.71
2.3	1.35	1.28	1.16	1.17	2.28	2.14	1.93	1.94	1.85	1.78	1.63	1.63
2.4	1.26	1.19	1.08	1.10	2.18	2.05	1.85	1.85	1.77	1.70	1.55	1.55
2.5	1.18	1.11	1.03	1.01	2.09	1.94	1.77	1.75	1.70	1.61	1.49	1.47
2.6	1.12	1.05	0.95	0.95	2.00	1.87	1.69	1.67	1.63	1.56	1.42	1.40
2.7	1.04	0.98	0.90	0.88	1.91	1.79	1.61	1.59	1.55	1.48	1.35	1.33
2.8	0.99	0.93	0.84	0.82	1.84	1.69	1.55	1.53	1.50	1.41	1.31	1.28
2.9	0.92	0.87	0.78	0.78	1.74	1.63	1.47	1.47	1.42	1.36	1.24	1.23
3.0	0.86	0.80	0.72	0.73	1.66	1.56	1.40	1.40	1.35	1.29	1.18	1.17
3.1	0.79	0.75	0.68	0.67	1.59	1.50	1.35	1.33	1.29	1.24	1.14	1.11
3.2	0.73	0.69	0.64	0.63	1.53	1.41	1.29	1.27	1.24	1.17	1.09	1.06
3.3	0.69	0.66	0.60	0.60	1.47	1.35	1.24	1.22	1.20	1.12	1.04	1.02
3.4	0.66	0.62	0.58	0.56	1.42	1.30	1.18	1.16	1.15	1.08	0.99	0.97
3.5	0.63	0.59	0.53	0.52	1.36	1.25	1.13	1.11	1.11	1.04	0.95	0.92
3.6	0.60	0.55	0.50	0.49	1.32	1.21	1.10	1.08	1.07	1.01	0.92	0.90
3.7	0.55	0.50	0.46	0.47	1.25	1.15	1.05	1.04	1.02	0.95	0.88	0.86

Depth (cm)	Total Absorbed Dose Rate (cGy/h)											
	$D_{W(TG-43)}$				$D_{L(TG-43)}$				$D_{L(Mod)}$			
	I	II	III	IV	I	II	III	IV	I	II	III	IV
3.8	0.51	0.47	0.43	0.43	1.21	1.10	1.00	0.98	0.98	0.91	0.84	0.82
3.9	0.50	0.46	0.41	0.40	1.15	1.08	0.96	0.95	0.93	0.89	0.81	0.80
4.0	0.47	0.43	0.39	0.38	1.11	1.04	0.92	0.91	0.90	0.86	0.78	0.76
4.1	0.43	0.41	0.37	0.36	1.08	0.99	0.89	0.87	0.87	0.82	0.75	0.73
4.2	0.40	0.38	0.35	0.34	1.03	0.96	0.88	0.83	0.83	0.80	0.74	0.69
4.3	0.38	0.35	0.33	0.32	1.01	0.92	0.83	0.81	0.82	0.76	0.70	0.67
4.4	0.36	0.34	0.31	0.29	0.97	0.88	0.80	0.78	0.79	0.73	0.67	0.66
4.5	0.34	0.32	0.29	0.28	0.92	0.85	0.76	0.75	0.75	0.71	0.64	0.63
4.6	0.32	0.30	0.27	0.27	0.90	0.81	0.72	0.72	0.73	0.67	0.61	0.60
4.7	0.31	0.28	0.26	0.25	0.86	0.80	0.70	0.69	0.70	0.66	0.59	0.58
4.8	0.29	0.27	0.25	0.24	0.83	0.76	0.68	0.67	0.67	0.63	0.57	0.56
4.9	0.27	0.25	0.23	0.22	0.79	0.72	0.65	0.64	0.64	0.60	0.55	0.54
5.0	0.26	0.24	0.22	0.21	0.76	0.70	0.64	0.62	0.62	0.58	0.54	0.52

Table 4: Total absorbed dose rate ($cGy.h^{-1}$) as function of distance for different configurations of ^{103}Pd seeds in water and lung environments calculated by equation 1.

Depth (cm)	Total Absorbed Dose Rate (cGy/h)											
	$D_{W(TG-43)}$				$D_{L(TG-43)}$				$D_{L(Mod)}$			
	I	II	III	IV	I	II	III	IV	I	II	III	IV
0.1	21.4	21.0	17.8	22.5	36.9	35.0	27.0	33.8	21.1	20.9	17.0	21.4
0.2	21.0	20.8	19.2	22.1	34.7	33.4	28.3	32.7	19.8	19.9	17.8	20.6
0.3	19.7	19.7	20.1	20.9	33.4	31.5	29.8	31.9	19.1	18.8	18.7	20.2
0.4	18.7	18.2	18.6	18.8	31.6	29.9	28.8	29.5	18.1	17.8	18.1	18.6
0.5	**16.9**	**16.9**	**17.0**	**16.9**	**29.7**	**28.3**	**26.9**	**26.8**	**16.9**	**16.9**	**16.9**	**16.9**
0.6	15.5	15.2	15.0	15.1	27.7	26.5	25.3	25.7	15.8	15.8	15.9	16.2
0.7	14.3	13.8	13.4	13.5	26.9	25.16	23.3	23.7	15.4	15.0	14.6	14.9
0.8	12.6	12.5	11.9	12.1	25.1	23.3	21.6	22.1	14.3	13.9	13.6	14.0
0.9	11.5	10.9	10.6	10.6	23.0	21.2	20.2	19.6	13.1	12.6	12.7	12.3
1.0	10.2	9.85	9.35	9.46	21.7	19.8	18.5	18.6	12.4	11.8	11.6	11.7
1.1	9.41	8.83	8.19	8.42	20.3	18.5	17.3	16.9	11.6	11.0	10.9	10.7
1.2	8.37	7.82	7.36	7.58	19.2	17.4	15.9	16.2	11.0	10.4	10.0	10.2
1.3	7.50	6.95	6.67	6.56	18.1	16.0	15.0	15.1	10.3	9.61	9.45	9.55
1.4	6.88	6.28	5.98	5.90	17.1	15.5	14.1	14.1	9.80	9.29	8.85	8.94
1.5	6.22	5.74	5.28	5.26	16.1	14.6	13.3	13.2	9.21	8.76	8.41	8.35
1.6	5.52	5.14	4.69	4.72	15.2	13.9	12.2	12.4	8.74	8.32	7.69	7.84
1.7	5.08	4.70	4.15	4.28	14.2	12.9	11.5	11.6	8.15	7.71	7.24	7.35

Depth (cm)	Total Absorbed Dose Rate (cGy/h)											
	$D_{W(TG-43)}$				$D_{L(TG-43)}$				$D_{L(Mod)}$			
	I	II	III	IV	I	II	III	IV	I	II	III	IV
1.8	4.57	4.22	3.82	3.87	13.7	12.1	10.8	10.8	7.87	7.26	6.84	6.88
1.9	3.92	3.79	3.50	3.40	12.7	11.5	10.3	10.5	7.28	6.88	6.51	6.65
2.0	3.58	3.44	3.09	3.11	12.0	10.9	9.53	9.63	6.89	6.52	5.98	6.09
2.1	3.29	3.07	2.75	2.90	11.2	10.2	9.01	9.26	6.44	6.11	5.66	5.85
2.2	3.04	2.77	2.50	2.62	10.7	9.63	8.73	8.95	6.16	5.75	5.48	5.65
2.3	2.82	2.55	2.25	2.30	10.0	9.34	8.10	8.16	5.73	5.58	5.08	5.15
2.4	2.54	2.30	2.02	2.08	9.65	8.53	7.59	7.67	5.51	5.10	4.77	4.85
2.5	2.12	2.10	1.83	1.90	9.15	8.31	7.32	7.25	5.23	4.96	4.60	4.58
2.6	1.99	1.91	1.69	1.74	8.82	7.94	6.86	6.98	5.04	4.75	4.31	4.41
2.7	1.93	1.64	1.61	1.59	8.17	7.27	6.71	6.69	4.67	4.34	4.21	4.23
2.8	1.61	1.56	1.42	1.49	7.63	6.92	6.27	6.35	4.36	4.14	3.93	4.01
2.9	1.47	1.43	1.25	1.28	7.30	6.60	5.87	5.83	4.17	3.94	3.68	3.68
3.0	1.34	1.29	1.12	1.15	6.90	6.35	5.60	5.57	3.94	3.79	3.51	3.52
3.1	1.26	1.12	1.07	1.04	6.66	6.00	5.33	5.17	3.81	3.58	3.34	3.27
3.2	1.18	1.00	0.93	0.97	6.28	5.78	4.94	5.11	3.59	3.45	3.10	3.23
3.3	1.04	0.93	0.83	0.90	6.13	5.41	4.77	4.83	3.50	3.23	2.99	3.05
3.4	0.95	0.85	0.81	0.80	5.96	5.07	4.66	4.62	3.41	3.03	2.93	2.92
3.5	0.90	0.78	0.72	0.73	5.78	4.93	4.50	4.48	3.30	2.94	2.83	2.83
3.6	0.79	0.76	0.65	0.70	5.39	4.73	4.36	4.14	3.08	2.83	2.74	2.61
3.7	0.71	0.67	0.62	0.58	5.12	4.56	4.02	4.04	2.93	2.72	2.52	2.55
3.8	0.65	0.61	0.54	0.52	4.91	4.23	3.83	3.82	2.80	2.52	2.40	2.41
3.9	0.62	0.57	0.51	0.46	4.74	4.16	3.74	3.56	2.71	2.48	2.35	2.25
4.0	0.59	0.49	0.48	0.42	4.53	4.00	3.52	3.21	2.59	2.39	2.21	2.03
4.1	0.54	0.48	0.45	0.41	4.20	3.87	3.39	3.11	2.40	2.31	2.13	1.97
4.2	0.44	0.43	0.39	0.42	4.06	3.56	3.18	3.04	2.32	2.13	2.00	1.92
4.3	0.44	0.36	0.38	0.37	3.98	3.39	3.03	3.08	2.27	2.02	1.90	1.95
4.4	0.45	0.34	0.34	0.32	3.77	3.21	2.91	2.84	2.15	1.91	1.82	1.79
4.5	0.43	0.30	0.30	0.30	3.57	3.06	2.74	2.89	2.04	1.83	1.72	1.83
4.6	0.36	0.29	0.27	0.27	3.43	3.00	2.57	2.62	1.96	1.79	1.61	1.65
4.7	0.29	0.28	0.24	0.22	3.26	2.85	2.49	2.65	1.86	1.70	1.56	1.67
4.8	0.28	0.23	0.22	0.21	2.98	2.75	2.47	2.44	1.70	1.64	1.55	1.54
4.9	0.27	0.22	0.23	0.20	2.92	2.64	2.22	2.16	1.67	1.58	1.40	1.37
5.0	0.22	0.20	0.22	0.19	2.87	2.49	2.22	2.08	1.64	1.49	1.39	1.31

$D_{L(Mod)}$. Tables 3 and 4 illustrate total absorbed dose rates ($cGy.h^{-1}$) as function of distance for different configurations of ^{125}I and ^{103}Pd seeds calculated by using TG-43 protocol-based and modified source strength. In a study conducted by Chen [9], the mean radioactivity per seed were 0.48, 0.52, 0.44 and 0.39 mCi / seed for configurations I, II, III and IV of ^{125}I seeds, respectively. The differences between modified source strength presented in

this study and Chen's study are 0%, -15.4%, -27.3% and -33.4% for mentioned arrangements, respectively. Another study conducted by Sutherland has reported modified radioactivities of 0.47, 0.43, 0.34 and 0.27 mCi / seed for configurations I, II, III and IV of ^{125}I seeds, respectively. The differences between modified source strength presented in this study and Sutherland's study [16] are 2.1%, 2.3%, -5.9% and -3.7% for mentioned configurations of ^{125}I seeds, respectively. In the following, dose differences at other depths in water and lung environments were calculated by equation 2 and were compared to each other in a 5 cm distance. As it is seen in Table 5, if modified source strength were used in lung environment, the lung absorbed dose would modify -18.64%, -16.98%, -15.79% and -16.13% for configurations I, II, III and IV of ^{125}I seeds, respectively. For ^{103}Pd sources, this reduction is -42.82%, -40.24%, -37.18% and -36.79% for mentioned configurations, respectively (in the case of ^{103}Pd, the modification of prescription dose is almost 2 times more than ^{125}I). $D_{L(TG-43)}$ vs. $D_{W(TG-43)}$ and $D_{L(Mod)}$ vs. $D_{W(TG-43)}$ were compared at further depths (beyond the prescription point) and the ratio of D_L/D_W was obtained at different depths. It is seen that the ratio of D_L/D_W is a quadratic function of depth ($D_L/D_W = a_1(d)^2 + a_2(d) + a_3$). This ratio is greater when protocol-based source strength is used for both environments and becomes less in the case of using modified source strength for lung. However, this ratio is constantly a quadratic function of depth for all configurations of ^{125}I and ^{103}Pd seeds. All equations presented in Table 5 were obtained by curve fitting with $R^2>0.99$. Because the equations of each column (Table 5) had close coefficients, the average of coefficients was used to obtain one equation for four configurations of seeds. Hence, for different configurations of ^{125}I seeds, $D_{L(TG-43)} / D_{W(TG-43)}$ gives a polynomial equation of grade two with $a_1 = 0.045$, $a_2 = 0.13$ and $a_3 = 1.13$. The ratio $D_{L(Mod)} / D_{W(TG-43)}$ gives another depth-dependent quadratic equation with $a_1 = 0.037$, $a_2 = 0.11$ and $a_3 = 0.94$. These equations are shown in Figure 4. In addition, for different configurations of ^{103}Pd seeds, $D_{L(TG-43)} / D_{W(TG-43)}$ gives a polynomial equation of grade two with $a_1 = 0.43$, $a_2 = -0.24$ and $a_3 = 1.85$ and $D_{L(Mod)} / D_{W(TG-43)}$ gives similar equation with $a_1 = 0.26$,

Table 5: Percentage dose difference in lung (%Diff [$D_{L(Mod)}$: $D_{L(TG-43)}$]) due to modification of source strength; and the ratio of lung-water absorbed dose (D_L/D_W) in cases of using protocol and modified source strength for different configurations of ^{125}I and ^{103}Pd seeds.

	Seeds	%Diff [$D_{L(Mod)}$: $D_{L(TG-43)}$]	$D_{L(TG-43)} / D_{W(TG-43)}$	$D_{L(Mod)} / D_{W(TG-43)}$
	^{125}I			
I	40	- 18.64 %	= 0.046 (d)2 + 0.13 (d) + 1.16	= 0.038 (d)2 + 0.10 (d) + 0.94
II	40	- 16.98 %	= 0.045 (d)2 + 0.13 (d) + 1.13	= 0.038 (d)2 + 0.11 (d) + 0.94
III	50	- 15.79 %	= 0.041 (d)2 + 0.14 (d) + 1.11	= 0.035 (d)2 + 0.12 (d) + 0.94
IV	60	- 16.13 %	= 0.047 (d)2 + 0.12 (d) + 1.12	= 0.039 (d)2 + 0.10 (d) + 0.94
	^{103}Pd			
I	40	- 42.82 %	= 0.41 (d)2 - 0.13 (d) + 1.84	= 0.23 (d)2 - 0.07 (d) + 1.05
II	40	- 40.24 %	= 0.51 (d)2 - 0.58 (d) + 2.12	= 0.30 (d)2 - 0.34 (d) - 1.26
III	50	- 37.18 %	= 0.33 (d)2 + 0.14 (d) + 1.50	= 0.21 (d)2 + 0.09 (d) + 0.94
IV	60	- 36.79 %	= 0.47 (d)2 - 0.41 (d) + 1.94	= 0.30 (d)2 - 0.26 (d) + 1.23

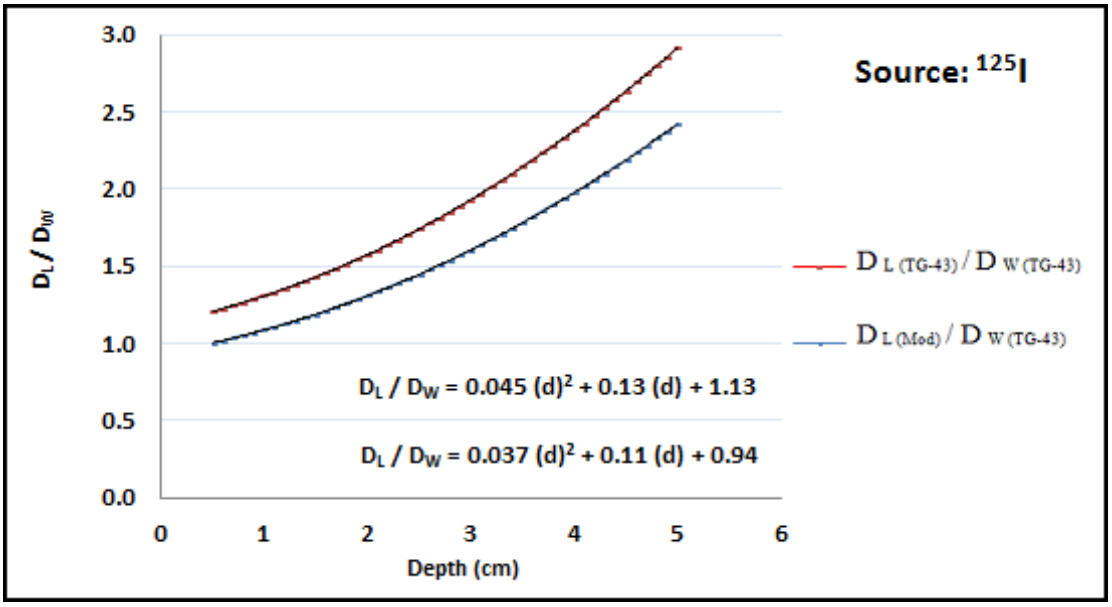

Figure 4: The ratio of D_L/D_W as function of depth for different configurations of ^{125}I seeds. The average of coefficients in Table 5 were used to obtain a single equation for each case.

a_2 = -0.14 and a_3 = 1.01, as well. These equations are shown in Figure 5.

Based on results, it is obvious that a simple change (modification) in source strength for the prescription point cannot eliminate the depth-dependent differences between lung and water absorbed doses at other depths. Therefore, in addition to modified strength, the equations presented in Figures 4 and 5 should also be considered. Due to the impossibility of dosimetry in actual lung and protocol-based calculation limitations, lung absorbed dose at different depths can be obtained directly from $D_{W(TG-43)}$ by mentioned equations. Dose differences between two environments result from particle transport and dose scoring. Due to the difference of water-lung electron densities (4:1), photon energy fluence is higher at deeper distances in lung environment. Energy absorbed per unit energy fluence and Roentgen-to-Rad conversion factors are other factors that cause differences between lung and water. Roentgen-to-Rad conversion factor is a function of material composition and photon energy. As regards to the results, it seems that the coincidence of these factors leads to a depth-dependent quadratic difference. It is necessary to point that these results are based on plane phantom geometry considering no deformation; while in reality there is sometimes seeds disarrangement or mesh deformation which can lead to asymmetric dose distribution and hot spots. In addition, although each single source was validated and benchmarked by the authors, inaccessibility to realistic patient data set restricts us to see how the presence of artifacts or tissue density (e.g. ribs) affects the dose distribution. On the other hand, at low energies like this, it is not clear yet how to specify dose to a medium (as dose to water in the medium). Therefore, Monte Carlo method is a unique way to calculate the absorbed dose with high accuracy in lung LDR brachytherapy. Another point is that using Monte Carlo method with accurate simulation of brachytherapy seeds can take some missing into consideration; interested effects and attenuation/changing of initially emitted photon that would not be considered through protocol-based point/line source calculations.

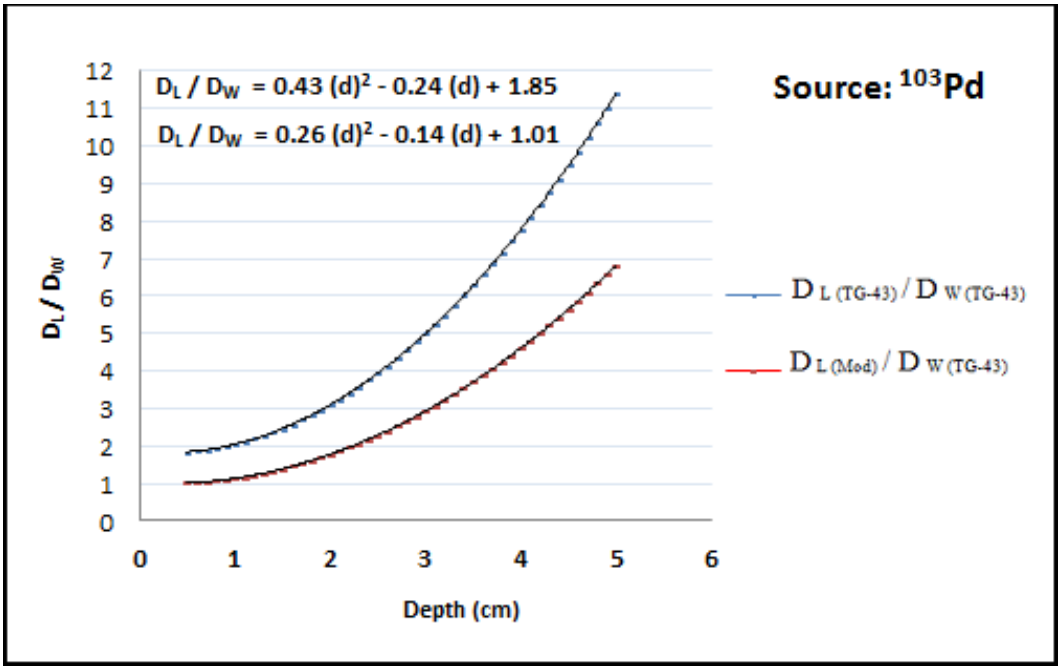

Figure 5: The ratio of D_L/D_W as function of depth for different configurations of ^{103}Pd seeds. The average of coefficients in table 5 were used to obtain a single equation for each case.

Conclusion

Different configurations of ^{125}I and ^{103}Pd brachytherapy sources which are used in lung permanent implantation were studied by Monte Carlo method in this research. Using AAPM TG-43U1 recommendations, protocol-based source strength was calculated to deliver recommended prescription dose in the water-equivalent environment. Lung absorbed dose was also calculated by mentioned source strength. Due to significant differences, protocol-based initial source strengths (initial air-kerma strength) were modified by the present authors for different configurations of ^{125}I and ^{103}Pd seeds so that prescription dose differences reached almost zero. However, further calculations at other depths indicated depth-dependent differences between lung and water environments in spite of prescription dose modifications. Therefore, several quadratic equations were obtained for different cases in form of $D_L/D_W = a_1(d)^2 + a_2(d) + a_3$ where D and d are absorbed dose and depth, respectively. Since the specification of dose to medium at low energies is not clear yet, and dosimetry in the actual lung is impractical, Monte Carlo method is a unique way of calculating absorbed dose, especially in LDR brachytherapy. Modified source strength and quadratic equations presented in this study are recommended to be considered in future studies based on lung permanent implant brachytherapy.

Acknowledgment

Authors would like to thank vice-chancellery for research and technology affairs of Shiraz University of Medical Sciences (SUMS) for supporting this research.

Conflict of Interest

There is not any relationship that might lead to a conflict of interest.

References

1. Jemal A, Siegel R, Ward E, Murray T, Xu J, Thun MJ. Cancer statistics, 2007. *CA Cancer J Clin.*

2007;**57**:43-66. doi.org/10.3322/canjclin.57.1.43. PubMed PMID: 17237035.

2. Lal R, Enting D, Kristeleit H. Systemic treatment of non-small-cell lung cancer. *European Journal of Cancer*. 2011;**47**:S375-S7. doi.org/10.1016/S0959-8049(11)70209-X.
3. Devlin PM. Brachytherapy: applications and techniques: Springer Publishing Company; 2015.
4. Voynov G, Heron DE, Lin CJ, Burton S, Chen A, Quinn A, et al. Intraoperative (125)I Vicryl mesh brachytherapy after sublobar resection for high-risk stage I non-small cell lung cancer. *Brachytherapy*. 2005;**4**:278-85. doi.org/10.1016/j.brachy.2005.03.007. PubMed PMID: 16344258.
5. Sutherland JG, Furutani KM, Thomson RM. Monte Carlo calculated doses to treatment volumes and organs at risk for permanent implant lung brachytherapy. *Phys Med Biol*. 2013;**58**:7061-80. doi.org/10.1088/0031-9155/58/20/7061. PubMed PMID: 24051987.
6. Sutherland J, Furutani K, Garces YI, Thomson R. Model-based dose calculations for 125I lung brachytherapy. *Med Phys*. 2012;**39**:4365-77. doi.org/10.1118/1.4729737. PubMed PMID: 24387504.
7. S Sutherland JG, Miksys N, Furutani KM, Thomson RM. Metallic artifact mitigation and organ-constrained tissue assignment for Monte Carlo calculations of permanent implant lung brachytherapy. *Med Phys*. 2014;**41**:011712. doi.org/10.1118/1.4851555. PubMed PMID: 24387504.
8. Johnson M, Colonias A, Parda D, Trombetta M, Gayou O, Reitz B, et al. Dosimetric and technical aspects of intraoperative I-125 brachytherapy for stage I non-small cell lung cancer. *Phys Med Biol*. 2007;**52**:1237-45. doi.org/10.1088/0031-9155/52/5/002. PubMed PMID: 17301451.
9. Chen A, Galloway M, Landreneau R, d'Amato T, Colonias A, Karlovits S, et al. Intraoperative 125I brachytherapy for high-risk stage I non-small cell lung carcinoma. *Int J Radiat Oncol Biol Phys*. 1999;**44**:1057-63. doi.org/10.1016/S0360-3016(99)00133-9. PubMed PMID: 10421539.
10. Venselaar J, Meigooni AS, Baltas D, Hoskin PJ. Comprehensive brachytherapy: physical and clinical aspects. Taylor & Francis: 2012.
11. Santos R, Colonias A, Parda D, Trombetta M, Maley RH, Macherey R, et al. Comparison between sublobar resection and 125Iodine brachytherapy after sublobar resection in high-risk patients with Stage I non-small-cell lung cancer. *Surgery*. 2003;**134**:691-7; discussion 7. doi.org/10.1016/S0039-6060(03)00327-1. PubMed PMID: 14605631.
12. Rivard MJ, Coursey BM, DeWerd LA, Hanson WF, Huq MS, Ibbott GS, et al. Update of AAPM Task Group No. 43 Report: A revised AAPM protocol for brachytherapy dose calculations. *Med Phys*. 2004;**31**:633-74. doi.org/10.1118/1.1646040. PubMed PMID: 15070264.
13. Rivard MJ, Butler WM, DeWerd LA, Huq MS, Ibbott GS, Meigooni AS, et al. Supplement to the 2004 update of the AAPM Task Group No. 43 Report. *Med Phys*. 2007;**34**:2187-205. doi.org/10.1118/1.2736790. PubMed PMID: 17654921.
14. Measurements ICRU. Determination of absorbed dose in a patient irradiated by beams of x or gamma rays in radiotherapy procedures. International Commission on Radiation Units and Measurements (ICRUM:24): Washington DC; 1976.
15. Van Dyk J, Keane TJ, Kan S, Rider WD, Fryer CJ. Radiation pneumonitis following large single dose irradiation: a re-evaluation based on absolute dose to lung. *Int J Radiat Oncol Biol Phys*. 1981;**7**:461-7. doi.org/10.1016/0360-3016(81)90131-0. PubMed PMID: 7251416.
16. Sutherland JG. Monte Carlo dose calculations for breast and lung permanent implant brachytherapy: Carleton University Ottawa; 2013.
17. Meigooni AS. Dosimetry of interstitial brachytherapy sources: Recommendations of the AAPM Radiation Therapy Committee Task Group No. 43. *Medical physics*. 1995;**22**:2.
18. Taylor RE, Yegin G, Rogers DW. Benchmarking brachydose: Voxel based EGSnrc Monte Carlo calculations of TG-43 dosimetry parameters. *Med Phys*. 2007;**34**:445-57. doi.org/10.1118/1.2400843. PubMed PMID: 17388160.
19. Woodard HQ, White DR. The composition of body tissues. *Br J Radiol*. 1986;**59**:1209-18. doi.org/10.1259/0007-1285-59-708-1209. PubMed PMID: 3801800.
20. White DR, Woodard HQ, Hammond SM. Average soft-tissue and bone models for use in radiation dosimetry. *Br J Radiol*. 1987;**60**:907-13. doi.org/10.1259/0007-1285-60-717-907. PubMed PMID: 3664185.
21. Mostaghimi H, Mehdizadeh AR, Darvish L, Akbari S, Rezaei H. Mathematical formulation of 125 I seed dosimetry parameters and heterogeneity correction in lung permanent implant brachytherapy. Journal of Cancer Research and Therapeutics. 2017. [in Press]
22. Rivard MJ. Monte Carlo radiation dose simulations

and dosimetric comparison of the model 6711 and 9011 I125 brachytherapy sources. *Medical physics*. 2009;**36**:486-91. doi.org/10.1118/1.3056463.

23. Dolan J, Li Z, Williamson JF. Monte Carlo and experimental dosimetry of an I125 brachytherapy seed. *Medical physics*. 2006;**33**:4675-84. doi.org/10.1118/1.2388158. PubMed PMID: 17278820.
24. Zabihzadeh M, Rezaee H, Shakarami Z, Feghhi M, Hosseini M. Dosimetric Characteristics of 103 Pd (Theragenices, Model 200) Brachytherapy Source. *Biomed Pharmacol*. 2015;**8**:15-23. doi. org/10.13005/bpj/550.